



## Article

# Enhancing Strength and Corrosion Resistance of Steel-Reinforced Concrete: Performance Evaluation of ICRETE Mineral Additive in Sustainable Concrete Mixes with PFA and GGBS

Kowshika V.R.<sup>1</sup>, Vijaya Bhaskaran<sup>1</sup>, Ramkumar Natarajan<sup>2</sup> and Iman Faridmehr<sup>3,\*</sup>

<sup>1</sup> International School of Management Excellence, Research Centre Affiliated to University of Mysore, Mysuru 570006, India; vr.kowshika@qcreteindia.com (K.V.); drvijayabaskaran@gmail.com (V.B.)

<sup>2</sup> Navoday Sciences Private Limited, Udaipur 313001, India; mkt@ecomaterials.com

<sup>3</sup> Civil Engineering Department, Faculty of Engineering, Girne American University, North Cyprus via Mersin 10, Kyrenia 99320, Turkey

\* Correspondence: imanfaridmehr@gau.edu.tr

**Abstract:** This study investigates the impact of an innovative mineral additive, ICRETE, on steel-reinforced concrete's compressive strength and corrosion resistance. Nineteen concrete mixes were designed incorporating recycled industrial by-products, including Ground Granulated Blast Furnace Slag (GGBS) and Pulverized Fuel Ash (PFA), with varying dosages of ICRETE. Compressive strength was tested using cube specimens, cured, and assessed at 3, 7, and 28 days following IS 516-2018 standards. Corrosion behavior was evaluated in accordance with ASTM G109, employing macrocell potential monitoring and electrochemical methods, including Tafel extrapolation and linear polarization resistance. The results revealed that ICRETE-enhanced mixes achieved compressive strengths of 56.93 MPa at a water–cement ratio of 0.35 and 50.61 MPa at 0.38, surpassing the control mix's 50.9 MPa at 0.33. Microstructural analysis via X-ray diffraction (XRD) and scanning electron microscopy (SEM) showed that ICRETE improved hydration, reduced porosity, and refined the microstructure, contributing to more excellent durability. Meanwhile, results demonstrated that the ICRETE additive reduced corrosion rates, displaying lower corrosion current densities and higher polarization resistance values where the corrosion rate dropped from 0.01 mmpy in control samples to 0.0081 mmpy with ICRETE. Environmental assessments indicated that ICRETE could significantly lower CO<sub>2</sub> emissions, reducing up to 46.50 kg CO<sub>2</sub> per cubic meter of concrete. These findings highlight ICRETE's potential to enhance strength and durability, supporting its use in sustainable, eco-friendly concrete applications.

**Keywords:** water–cement ratio; sustainable concrete; innovative additive; ready-mix concrete; compressive strength; Microstructural analysis; cement reduction; CO<sub>2</sub> emissions; Ground Granulated Blast Furnace Slag (GGBS)



**Citation:** V.R., K.; Bhaskaran, V.; Natarajan, R.; Faridmehr, I. Enhancing Strength and Corrosion Resistance of Steel-Reinforced Concrete: Performance Evaluation of ICRETE Mineral Additive in Sustainable Concrete Mixes with PFA and GGBS. *Infrastructures* **2024**, *9*, 228. <https://doi.org/10.3390/infrastructures9120228>

Academic Editor: Chris Goodier

Received: 2 November 2024

Revised: 7 December 2024

Accepted: 9 December 2024

Published: 11 December 2024



**Copyright:** © 2024 by the authors. Licensee MDPI, Basel, Switzerland. This article is an open access article distributed under the terms and conditions of the Creative Commons Attribution (CC BY) license (<https://creativecommons.org/licenses/by/4.0/>).

## 1. Introduction

The construction industry has long recognized the critical role of concrete as the primary material for infrastructure development. The city's rapid expansion and urbanization drive demand for creative building techniques that improve concrete performance while having less adverse effects on the environment. Ready-mix concrete has gained popularity worldwide as the material of choice for several construction projects because of its dependable quality and ease of usage. However, conventional concrete mix designs—particularly those that follow the conventional water–cement (w/c) ratio law—often limit the possibility of innovation in obtaining high strength and sustainability. The advent of advanced chemical admixtures, especially polycarboxylic ether (PCE) polymers, has revolutionized

concrete technology, enabling significant reductions in water content while maintaining or even enhancing the mechanical properties of concrete [1].

The relationship between the w/c ratio and concrete strength, first established by Abrams in the early 20th century, remains a cornerstone of concrete mix design [2]. According to Abrams' law, a lower w/c ratio leads to higher compressive strength, which has guided the development of concrete mixes for decades. However, introducing modern admixtures and supplementary cementitious materials (SCMs) has increasingly challenged this principle. Recent studies have demonstrated that these additives can modify or defy traditional w/c ratio law [3–5]. For instance, research by Kondraivendhan and Bhattacharjee explored the relationship between pore structure and compressive strength, suggesting that certain admixtures could mitigate the effects of higher w/c ratios on strength [2]. Similarly, Hedegaard and Hansen tested fly ash concrete and showed that the classical w/c ratio law is valid, though with modifications to account for the unique properties of SCMs [6]. Other studies on microsilica and other pozzolanic materials also highlighted the potential for reducing cement content and water demand while maintaining high strength and durability [7–9]. These developments have opened new avenues for optimizing concrete mix designs, particularly in the context of sustainability and reducing the carbon footprint of concrete production.

In recent studies, the incorporation of mineral additives in concrete has gained substantial attention for improving both mechanical strength and corrosion resistance. Mehta and Monteiro [10] highlighted that the use of supplementary cementitious materials (SCMs) like fly ash and slag reduces the demand for Portland cement, contributing to both strength and sustainability improvements. The study demonstrated that fly ash enhances durability by reducing permeability and mitigating the effects of chloride penetration, which is critical for reinforced concrete exposed to aggressive environments. Similarly, Abbas et al. [11] investigated the application of nano-silica in concrete, reporting a significant improvement in compressive strength and microstructural densification, which enhanced corrosion resistance. On the same topic, Q Fu et al. [12] evaluated the effectiveness of incorporating silica fume in concrete mixtures, finding that it not only improved the mechanical properties but also reduced the risk of steel rebar corrosion by decreasing the porosity of the concrete. Additionally, the study by AS Gill et al. [13] examined the long-term performance of ground granulated blast furnace slag (GGBS) in concrete, confirming that GGBS significantly improves concrete's durability and corrosion resistance, especially under sulfate-rich conditions.

Despite significant advancements in enhancing concrete's strength and durability using various mineral additives, a research gap persists in understanding the combined impact of innovative additives on compressive strength and corrosion resistance across different concrete grades. To address this gap, this study aims to evaluate the dual benefits of ICRETE, a novel mineral additive, in improving strength and durability while promoting sustainability. The research involves a comprehensive series of experiments with different concrete mixes, incorporating Ordinary Portland Cement (OPC), Ground Granulated Blast Furnace Slag (GGBS), and Pulverized Fuel Ash (PFA) with varying dosages of ICRETE. These mixes were subjected to compressive strength testing following IS 516-2018 standards [14] and corrosion assessments according to ASTM G109 guidelines, utilizing macrocell potential monitoring and electrochemical techniques. This methodology allows for a detailed evaluation of ICRETE's effectiveness in enhancing concrete performance under diverse conditions, filling the existing research gap.

## 2. Materials and Methods

### 2.1. Materials

The experimental program was structured to assess the impact of the ICRETE across different types of concrete mixes, including OPC mixes, OPC combined with GGBS, and OPC mixed with PFA. These mix series were designated OPC Mix Series, OPC+GGBS Mix Series, OPC+PFA Series 1, and OPC+PFA Series 2. Each mix was designed according to the

guidelines outlined in IS 10262-2019 [15], which provides the standards for concrete mix proportioning. Additionally, the principles defined in IS 456-2000 [16], a code of practice for plain and reinforced concrete, were adhered to throughout the experimental process [17].

- **Aggregates:** This study utilized two varieties of coarse aggregates: 12.5 mm and down and 20 mm and down. The aggregates were chosen in compliance with IS 383-2016 [18], guaranteeing that they fulfilled structural concrete’s chemical and physical requirements [18]. The sieve analysis for both aggregates confirmed their compliance with the standard grading limits, with the larger aggregate showing a cumulative percent passing of 93.5% at the 20 mm sieve and the smaller aggregate showing 97.5% passing at the 12.5 mm sieve.

Figure 1 shows that the sieve analysis for both aggregates confirmed their compliance with the standard grading limits.

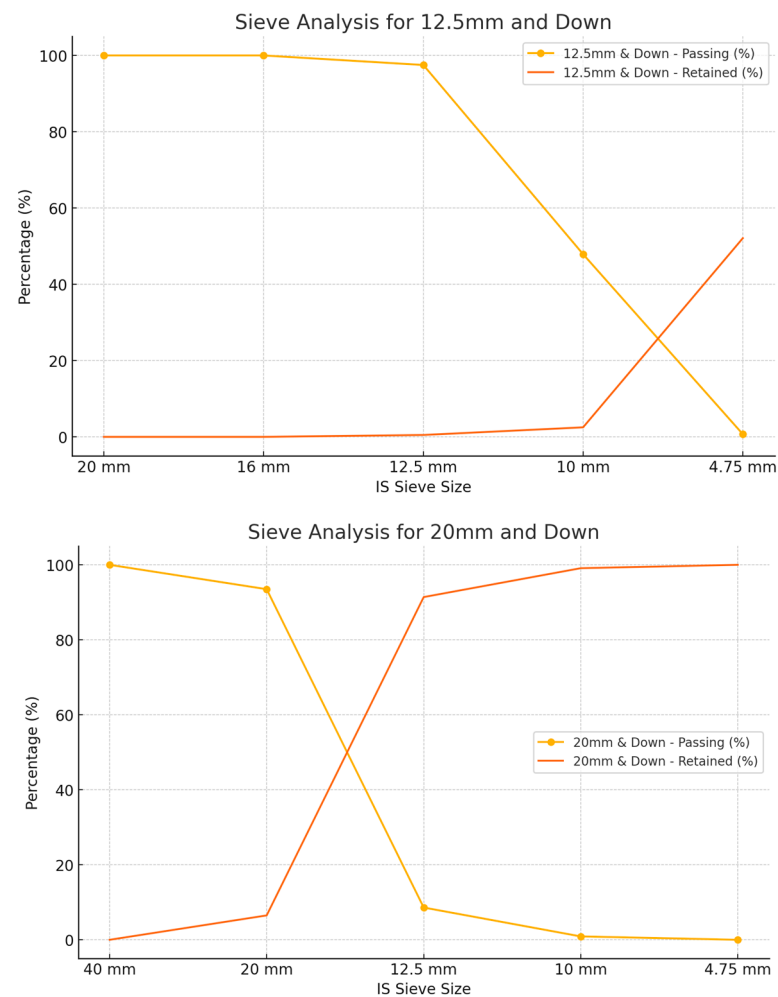


Figure 1. Sieve Analysis of Coarse Aggregate.

- **Crushed Stone Sand:** The crushed stone sand used as a fine aggregate was sourced from a crusher plant, meeting the quality standards of IS 383-2016. Despite the potential for a higher content of fine particles (up to 150 microns), the sand utilized in this study was within the permissible limits, confirming Zone II requirements as per the standard, as shown in Figure 2.

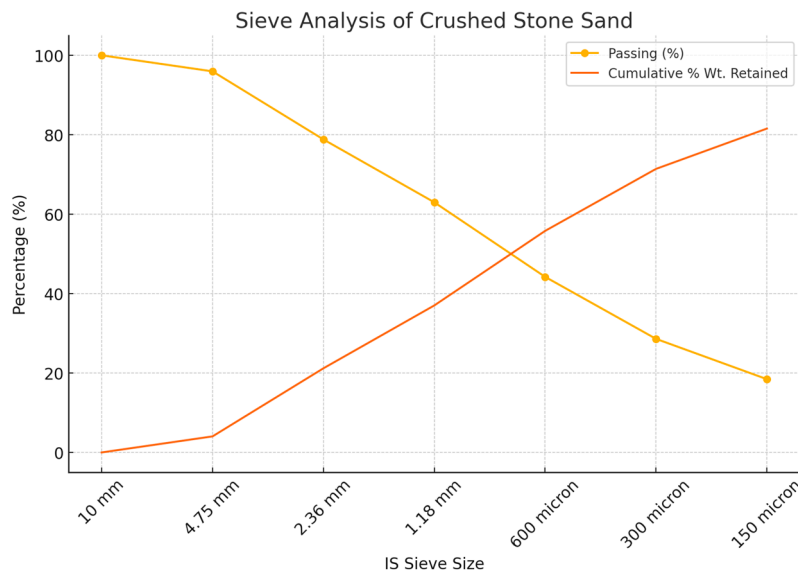


Figure 2. Sieve Analysis-Crushed Stone Sand.

- Cement: Dalmia 53 Grade OPC was selected for the study, widely recognized for its high strength and durability in ready-mix concrete applications. The cement’s chemical and physical properties were tested and found to comply with IS 269-2015 specifications [19]. Notable properties include a loss on ignition of 2.71%, an initial setting time of 140 min, and a compressive strength of 60.5 MPa at 28 days, exceeding the minimum requirement of 53 MPa. The cement’s chemical and physical properties were tested and found to comply with IS 269-2015 specifications, as detailed in Table 1 [20].

Table 1. Chemical and Physical Properties of OPC 56 grade Cement.

Sl No	Particulars	Test Results	Specifications as per IS:269:2015
A	Chemical Requirements		
1	Loss on Ignition, (% by mass)	2.71	Not More than 4%
2	Insoluble residue, (% by mass)	1.4	Max. 5.00%
3	Ratio of % of lime to % of Silica, Alumina and Iron Oxide, When Calculated by the formula	0.92	Not greater than 1.02 And not less than 0.8
4	Ratio of % of Alumina to that of Iron Oxide	1.14	Min. 0.66
5	Total sulfur Content Calculated as sulfuric anhydride (SO <sub>3</sub> ), (% by mass)	1.73	Max 3.5%
6	Magnesia (MgO), (% by mass)	1.01	Max 6.0%
7	Tricalcium Aluminate (C <sub>3</sub> A), (% by mass)	5.96	Not specified
8	Alkali Content (% by mass) (i) Alkalies as Na <sub>2</sub> O (ii) Alkalies as K <sub>2</sub> O (iii) Total alkalies as Na <sub>2</sub> O equivalent	0.18 0.42 0.46	In the case of reactive aggregate, the use of cement with alkali content below 0.6 percent expressed as sodium oxide (Na <sub>2</sub> O + 0.658K <sub>2</sub> O) is recommended
9	Chloride Content, (% by mass)	0.007	Max. 0.1% (0.05% for pre-stressed structures)
B	Physical Requirements		
1	Consistency	28%	Not specified
2	Initial Setting Time	140 min	Shall not be less than 30 min
3	Final Setting Time	275 min	Shall not be more than 600 min

**Table 1.** *Cont.*

Sl No	Particulars	Test Results	Specifications as per IS:269:2015
4	Compressive Strength		
	(a) 72 +/- 1 h (average of three results)	37.0 MPa	Shall not be less than 27.0 MPa
	(b) 168 +/- 2 h (average of three results)	46.5 MPa	Shall not be less than 37.0 MPa
	(c) 672 +/- 4 h (average of three results)	60.5 MPa	Shall not be less than 53.0 MPa
5	Fineness (by Blain’s air permeability method)	342 m <sup>2</sup> /kg	Shall not be less than 225 m <sup>2</sup> /kg
6	Soundness (by Le Chatelier’s Method)	0.5 mm	Shall not be more than 10 mm
7	Soundness (by Autoclave expansion method)	0.028%	Shall not be more than 0.8%

- Supplementary Cementitious Materials: GGBS and PFA were used as supplementary cementitious materials to partially replace OPC in some of the mixes. GGBS, characterized by a specific gravity of 2.84 and a specific surface area of 378 m<sup>2</sup>/kg, meets the IS 16714-2018 standard [21], with particular properties detailed in Table 2.

**Table 2.** Chemical and Physical Properties of GGBS.

Sl No	Characteristics	Test Results	Specifications as per IS:16714-2018
A	Chemical Requirements:		
1	Manganese Oxide (MnO) %	0.32	5.5 Max
2	Magnesium Oxide (MgO) %	7.88	17.0 Max
3	Sulfide Sulfur (S) %	0.52	2.0 Max
4	Sulfate (as SO <sub>3</sub> ) %	0.10	3.0 Max
5	Insoluble residue (I R) %	2.32	3.0 Max
6	Chloride Content (Cl) %	0.004	0.1 Max
7	Glass Content %	96.8	85 Min
8	Gain on Ignition %	0.16	Not Specified
9	$\frac{\text{CaO}+\text{MgO}+1/3\text{Al}_2\text{O}_3}{\text{SiO}_2+2/3\text{Al}_2\text{O}_3}$	1.09	1.0% (Min)
10	$\frac{\text{CaO}+\text{MgO}+\text{Al}_2\text{O}_3}{\text{SiO}_2}$	1.78	1.0% (Min)
B	Physical Requirements		
1	Specific Gravity	2.84	Not Specified
2	Specific Surface Area (M <sup>2</sup> /Kg)	378	320 (Min)
3	Slag Activity		
	(a) 7 Days	72.0	60% (Min)
	(b) 28 Days	91.0	75% (Min)

PFA, classified as Class F, was sourced from the Ennore thermal power plant, and it met the requirements of IS 3812-2013 [22]. The PFA exhibited a silicon dioxide content of 63.51%, with a Blaine fineness of 401 m<sup>2</sup>/kg. The PFA exhibited desirable properties, which are summarized in Table 3.

**Table 3.** Chemical and Physical Properties of PFA.

Test Conducted	Results	Requirements as per IS:3812:2013 (RA 2017)
Chemical		
Silicon dioxide (SiO <sub>2</sub> ) plus aluminum oxide (Al <sub>2</sub> O <sub>3</sub> ) plus iron oxide (Fe <sub>2</sub> O <sub>3</sub> ), Percent by mass (Minimum)	90.77%	70% (Siliceous)/50% (Calcareous)
Magnesium oxide (MgO), Percent by mass (Maximum)	1.81%	5%
Sulfur trioxide (SO <sub>3</sub> ), Percent by mass (Maximum)	0.10%	3%
Loss on ignition, Percent by mass (Maximum)	2.14%	5% (Siliceous)/7% (Calcareous)
Available alkalis as sodium oxide (Na <sub>2</sub> O) Percent by mass (Maximum)	0.79%	1.5%
Physical		
Specific Gravity	2.2	-
Fineness- Specific surface in (m <sup>2</sup> /kg) by Blaine’s Air-Permeability method	401	Minimum 320 (Siliceous)/200 (Calcareous)
Lime reactivity—Average Compressive Strength in N/mm <sup>2</sup>	5.8	Minimum 4.5
Soundness by Autoclave Test Expansion of Specimens, percent	0.028%	Maximum 0.8%
Residue on 45-micron sieve, percent	11.4%	Maximum 34% (Siliceous)/50% (Calcareous)

- Innovative Additive:** The innovative additive, ICRETE, used in this study is a precisely engineered, patented blend designed to enhance the performance of concrete by improving its mechanical properties and environmental sustainability. This additive is a blend of high-purity silica (SiO<sub>2</sub>), activated alumina (Al<sub>2</sub>O<sub>3</sub>), calcium carbonate (CaCO<sub>3</sub>), magnesium oxide (MgO), and organic dispersants. These components work synergistically to promote the formation of additional C-S-H phases during hydration, improve early-age strength development, and enhance durability. The tiny particle size distribution makes better interaction with cementitious materials possible, guaranteeing uniform dispersion throughout the concrete matrix. Its slightly alkaline pH level encourages ideal hydration without adversely influencing the setting time. The combination’s low moisture content guarantees optimal workability and reduced porosity while reducing the possibility of adding too much water. Table 4 lists the essential chemical and physical properties of the additive.

**Table 4.** Physical and Chemical Properties of Innovative Additive, ICRETE.

Parameter	Testing Protocol	Results
Silicon dioxide (SiO <sub>2</sub> )	ASTM C114	55.2%
Alumina (Al <sub>2</sub> O <sub>3</sub> )	ASTM C114	18.7%
Calcium carbonate (CaCO <sub>3</sub> )	ASTM C114	12.4%
Magnesium oxide (MgO)	ASTM C114	7.8%
Organic dispersants (Polycarboxylate ethers —PCEs)	Proprietary analysis	Trace
Particle size % by mass passing in a 45-micron sieve	ASTM C117	90.7%
Bulk Density (Loose) gm/cc	ASTM C110	0.71
pH in 10% solution at 28 °C	ASTM D1293	9.9
Moisture Content % by mass	ASTM C566	0.97%
Methylene Blue Value MBf (mg/gm)	ASTM C1779	1.7

### 2.2. Mix Proportioning and Experimental Design

The proportions of the concrete mixes in this study were calculated in compliance with IS 10262-2019 criteria, ensuring that each mix met the specifications required for its intended application, as shown in Table 5. Three types of tests were conducted: compressive strength, corrosion behavior as per ASTM G109, and corrosion behavior through electrochemical studies. The compressive strength was evaluated using 100 mm × 100 mm × 100 mm cube specimens, tested at intervals of 7, and 28 days following IS 516-2018 standards. Corrosion behavior, according to ASTM G109 [23], was assessed using 300 mm × 115 mm × 150 mm prism specimens, tested at various stages outlined by ASTM G109 guidelines. Additionally, corrosion behavior was examined through electrochemical studies using 50 mm × 100 mm cylindrical specimens, tested after 28 days of curing, and again at 6 months. This methodology was designed to explore the impact of different dosages of the ICRETE additive, focusing on optimizing concrete properties, reducing cementitious content, and maintaining or enhancing compressive strength across varying water–cement (w/c) ratios.

**Table 5.** Mix Series and Compressive Strength Results.

Mix Sample	Dosage of Innovative Additive	Mix Description								Avg. Strength (Mpa)	
		Cement (OPC)	GGBS or PFA	20 mm	12.5 mm	CSS	Water	Total CC	w/c	7 Day	28 Day
OPC Mix Series											
OP CON-1	0.0%	450	0	598	485	720	150	450	0.33	43.27	50.90
OPNA-1	0.8%	425	0	596	485	738	150	425	0.35	45.88	56.93
OPNA-2	1.2%	400	0	594	484	760	150	400	0.38	41.72	50.61
OPC+GGBS Mix Series											
OPGG CON-1	0.0%	225	225	590	477	718	150	450	0.33	33.53	41.41
OPGGNA-1	0.8%	212.5	212.5	590	480	730	150	425	0.35	42.71	50.90
OPGGNA-2	1.2%	200	200	580	471	766	150	400	0.38	36.30	43.24
OPGGNA-3	1.5%	188	188	584	475	778	150	375	0.4	38.24	44.52
OPGGNA-4	2.0%	175	175	582	473	800	150	350	0.43	37.16	44.09
OPC+PFA Mix Series 1											
OPFLY CON-1	0.0%	360	90	610	495	683	144	450	0.32	43.53	51.16
OPCFLYNA-1	0.8%	340	85	608	494	704	144	425	0.34	47.16	55.17
OPCFLYNA-2	1.2%	320	80	606	494	725	144	400	0.36	47.30	53.41
OPCFLYNA-3	1.5%	300	75	611	494	741	144	375	0.38	43.35	53.14
OPCFLYNA-4	2.0%	280	70	609	496	761	144	350	0.41	40.80	50.62
OPCFLYNA-5	2.0%	260	65	607	494	786	144	325	0.44	41.88	49.20
OPC+PFA Mix Series 2											
OPCFLYNA-2	0.0%	293	157	643	523	586	150	450	0.33	29.59	45.35
OPCFLYNA-6	0.8%	276	149	644	524	602	150	425	0.35	33.60	47.41
OPCFLYNA-7	1.2%	260	140	645	525	621	150	400	0.38	33.60	48.30
OPCFLYNA-8	1.5%	244	131	646	526	641	150	375	0.40	33.51	48.77
OPCFLYNA-9	2.0%	228	122	647	527	661	150	350	0.43	28.64	43.73

Figure 3 illustrates the preparation, casting, and compressive strength testing of concrete specimens used in this study.



**Figure 3.** Preparation, casting, and compressive strength testing of concrete specimens.

### 2.3. Macrocell Corrosion Test Procedure

The macrocell corrosion test was conducted to evaluate the corrosion resistance of steel reinforcement embedded in concrete with and without the ICRETE mineral additive [24]. This test adhered to ASTM G109 guidelines, targeting the behavior of specimens under chloride-induced corrosion conditions. Concrete prisms, measuring 300 mm × 115 mm × 150 mm, were cast with either cleaned or epoxy-coated steel rebars. Following a curing period, each specimen was equipped with a reservoir on top, containing a chloride solution to simulate a corrosive environment. This ensured consistent exposure of the concrete surface to the chloride medium, which is necessary for inducing and monitoring corrosion. The specimens were maintained at a controlled relative humidity of 50% to standardize the environmental conditions throughout the test. The macrocell current and potential were measured weekly using a voltmeter, which recorded the voltage across a 10 Ω resistor connected to the steel reinforcement. The corrosion current,  $I_{corr}$ , was calculated using the following equation:

$$I = V/R$$

where  $I$  is the current in amps,  $V$  is the measured voltage in volts, and  $R$  is the resistance, set at 10 Ω.

Additionally, the corrosion potential of the embedded steel was evaluated against a reference electrode following ASTM C876-22b standards [25]. This setup enabled a detailed assessment of the ICRETE additive’s ability to reduce corrosion by monitoring variations in current and potential over time, offering insights into its potential to enhance concrete durability for sustainable construction applications. Figure 4 shows an overview of the Macrocell Corrosion Testing Process, including steel rebar arrangement, mold preparation, hardened specimen, controlled humidity conditions, and the chloride exposure and corrosion monitoring setup.



**Figure 4.** Stages of Macrocell Corrosion Testing Setup for Concrete Specimens.

#### 2.4. Electrochemical Test for Corrosion Evaluation

Electrochemical studies were performed to evaluate the corrosion resistance of steel reinforcement embedded in concrete using a series of standard procedures [26]. Steel rebar specimens with a diameter of 12 mm and a length of 50 mm were embedded in concrete cylinders measuring 50 mm × 100 mm with a 20 mm cover. Prior to embedding, rebars were cleaned and fitted with lead wires for connection. The concrete cylinders were then cured, and the specimens were immersed in a 3% NaCl solution to simulate a chloride-rich environment, accelerating the corrosion process. In this research, two key electrochemical

methods were used to evaluate the corrosion resistance of steel reinforcement embedded in concrete:

- Linear Polarization Resistance (LPR) Measurements:

LPR measurements were conducted to determine the polarization resistance ( $R_p$ ), directly related to the corrosion rate [27]. The tests involved applying a small potential sweep of  $\pm 20$  mV from the open circuit potential (OCP) at a constant sweep rate of 60 mV/min. The setup used an electrochemical workstation, where the steel rebar embedded in concrete acted as the working electrode. The obtained  $R_p$  values indicated the steel's corrosion resistance, with higher  $R_p$  values signifying better protection against corrosion. This method allowed for a quick and non-destructive assessment of the corrosion rate within the concrete specimens.

- Electrochemical Impedance Spectroscopy (EIS):

EIS was performed to analyze the frequency response of the steel reinforcement embedded in concrete [28]. The tests covered a frequency range from 0.1 Hz to 10 kHz, capturing the system's impedance behavior across different frequencies. An electrochemical workstation with the same electrode setup as LPR was used to conduct these tests. The resulting impedance data provided information about the concrete's electrochemical properties, including resistance to charge transfer and the material's capacitive behavior.

Figure 5 shows the electrochemical testing setup for corrosion evaluation, including steel rebar preparation with lead wires, immersion of concrete specimens in 3% NaCl solution for electrochemical analysis, and the monitoring setup during electrochemical impedance spectroscopy and LPR measurements.



**Figure 5.** Electrochemical Testing Setup for Corrosion Evaluation.

### 3. Results and Discussion

#### 3.1. Effect of Additive on Compressive Strength

The 28-day compressive strength results for various concrete mixes, listed in Table 5, are presented in Figure 6. The control mix (OP CON-1) achieved a compressive strength of 50.9 MPa, serving as a baseline for comparison. In the OPC Mix Series, including the innovative additive at dosages of 0.8% and 1.2%, resulted in enhanced compressive strengths, with OPNA-1 reaching the highest value of 56.93 MPa. At the same time, OPNA-

2 showed a slight reduction to 50.61 MPa. The OPC+GGBS Mix Series exhibited a moderate decrease in compressive strength, ranging from 41.41 MPa (OPGG CON-1) to 44.52 MPa (OPGGNA-3). The OPC+PFA Mix Series showed varied results, peaking at 55.17 MPa for OPCFLYNA-1, with a general trend of declining strength as the additive dosage increased, culminating in a compressive strength of 43.73 MPa for OPCFLYNA-9. Overall, Figure 6 shows that although the novel additive can increase compressive strength in some mixes, its efficacy depends on the particular cementitious combination and dose; performance noticeably declines at higher dosages, especially in PFA blends.

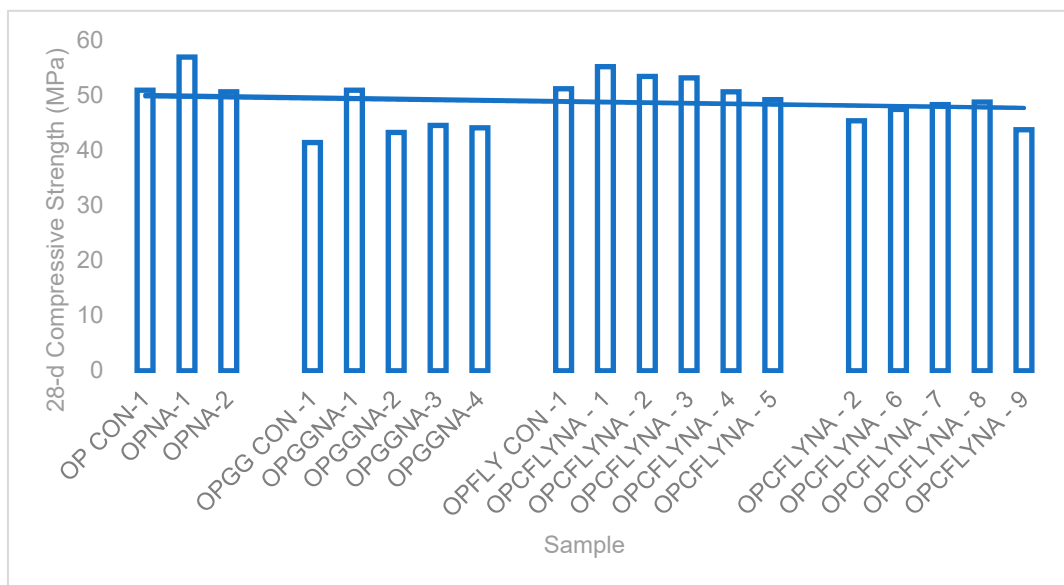


**Figure 6.** 28-Day Compressive Strength Results for Various Concrete Mixes Incorporating the Innovative Additive at Different Dosages.

Figure 7 shows the concrete compressive strength after 7- and 28-day periods with varying dosages of the novel additive. The orange and blue markers indicate compressive strengths for different additive dosages after 7 and 28 days, respectively. The trendlines suggest that compressive strength decreases slightly as the additive dosage increases. Additionally, the 28-day strength is generally higher than the 7-day strength. This indicates that within the tested range, the additive’s effect on strength is not significantly dependent on the dosage. The  $R^2$  values for the 28-day (0.0061) and 7-day (0.0038) compressive strengths show a weak relationship between additive dosage and compressive strength. This modest relationship suggests that other factors, such as the water-to-cement ratio, curing conditions, and the interaction between supplementary cementitious materials and the innovative additive, may be more critical in determining the concrete mixtures’ final compressive strengths. Overall, Figure 7 demonstrates that while the innovative additive impacts the compressive strength of the concrete, the dosage level within the tested range does not substantially influence the strength outcomes at either the 7-day or 28-day mark.

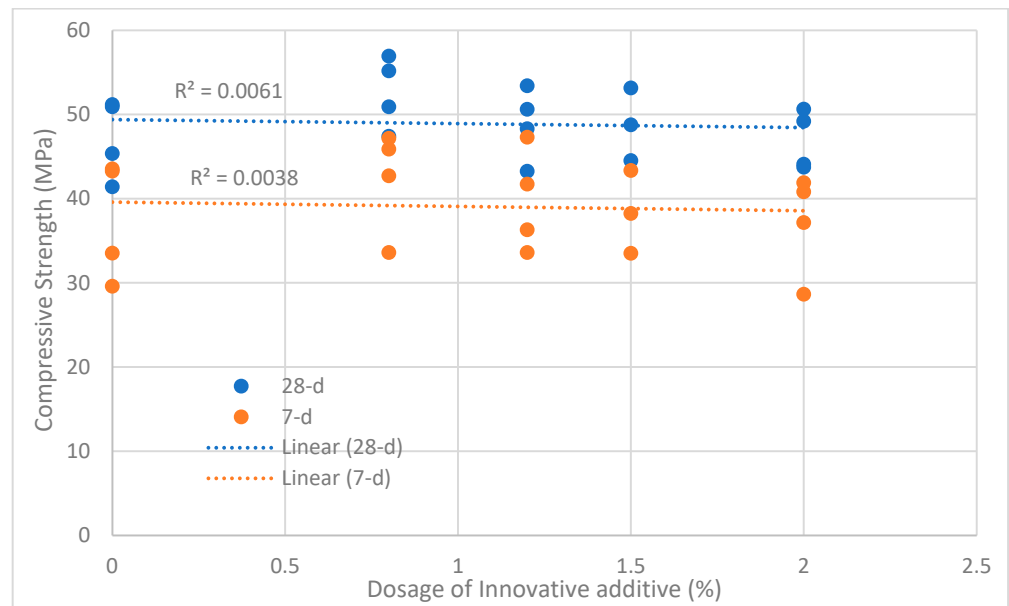


**Figure 7.** Relationship Between Dosage of Innovative Additive and Compressive Strength at 7-Day and 28-Day Intervals.

3.2. Effect of Additive on W/C Ratio

With an  $R^2$  value of 0.9064, the graph in Figure 8 illustrates the solid linear association between the dosage of the novel addition and the water–cement (w/c) ratio. The robust association indicated by the high  $R^2$  value implies that maintaining or improving the intended concrete qualities requires an increase in the dosage of the novel additive in proportion to the rise in the w/c ratio. The trendline clearly illustrates this proportionate relationship, emphasizing the need to carefully modify the additive dosage in response to changes in the w/c ratio. This proportionality also suggests that the additive effectively compensates for the potential strength reduction at higher W/C ratios, as demonstrated by the relatively stable compressive strengths in Table 5 despite varying W/C ratios. This connection is crucial for optimizing concrete mix designs since it guarantees that the mechanical properties do not degrade when the w/c ratio varies.

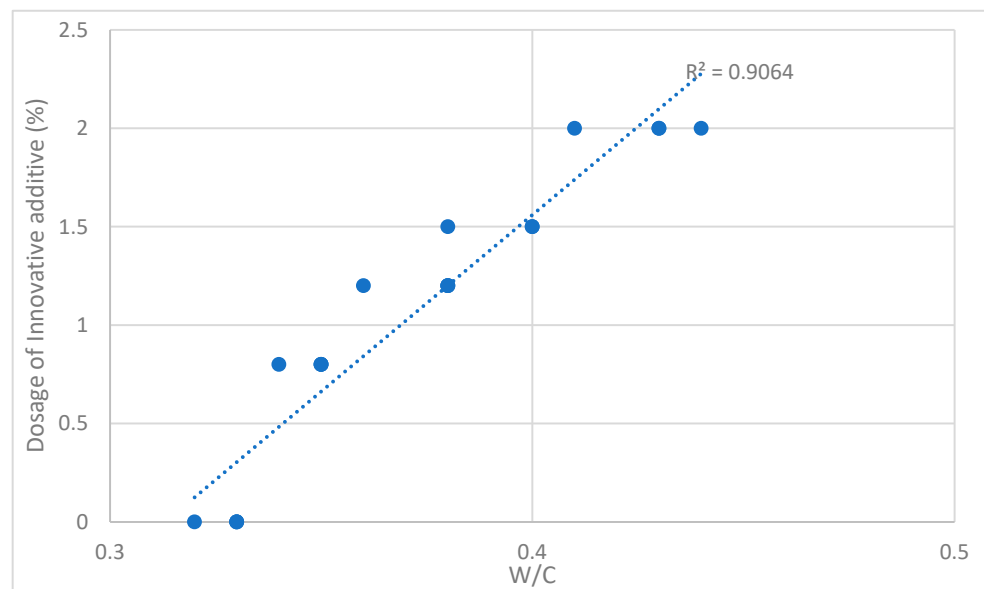


**Figure 8.** Relationship Between Water–Cement (W/C) Ratio and Dosage of Innovative Additive.

### 3.3. Microstructural Assessment

Selected specimens were subjected to XRD analysis to assess the novel additive's effect on the concrete's crystalline phases. The XRD patterns, Figure 9, shed light on the addition's microstructural variations in various concrete formulations.

The OPC+GGBS Mix Series specimen (OPGG CON-1), as shown in Figure 9a, displays prominent peaks associated with calcium hydroxide (CH) and calcium silicate hydrate (C-S-H) phases at different hydration stages (3, 7, and 28 days). The intensity of the CH peaks at 28 days suggests a typical hydration process with some remaining free lime content, which may affect durability. The CH peaks gradually decrease with time, implying that GGBS is causing a continual pozzolanic reaction that encourages the creation of more C-S-H phases and produces a more refined microstructure.

In contrast, the OPC+GGBS Mix Series specimen with 2% innovative additive (OPGGNA-4), depicted in Figure 9b, demonstrates a more pronounced reduction in CH peaks over the same time intervals (3, 7, and 28 days). The notable decline in CH seen on day 28 implies that the novel addition has quickened the pozzolanic reaction, which has increased CH consumption and furthered the production of advantageous C-S-H phases. As a result, the microstructure is denser and more resilient than the reference specimen's. Additionally, the overall intensity of the peaks indicates the formation of fewer crystalline phases, highlighting the role of the additive in promoting a more amorphous and stable hydration product.

The XRD analysis confirms that the innovative additive substantially influences the hydration process, reducing the formation of less desirable phases like CH while promoting the development of C-S-H.

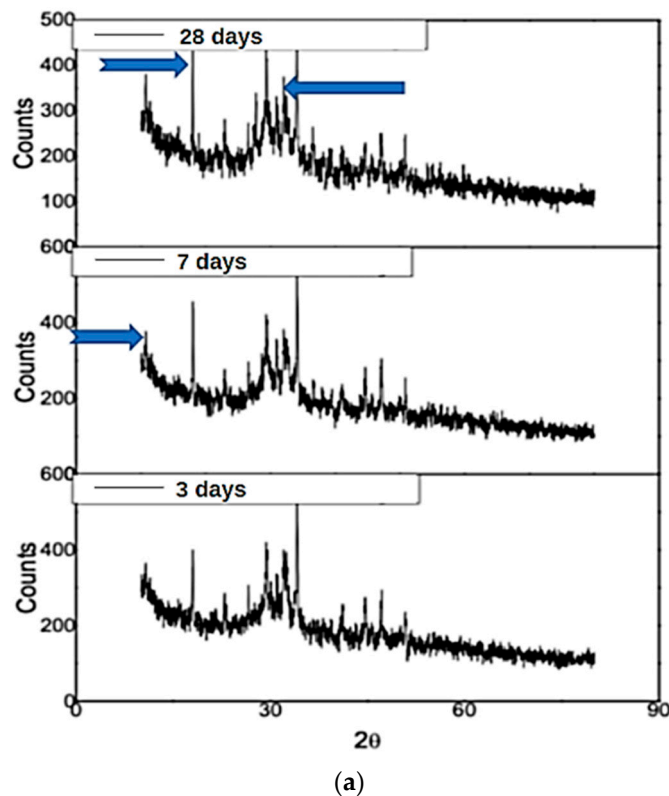
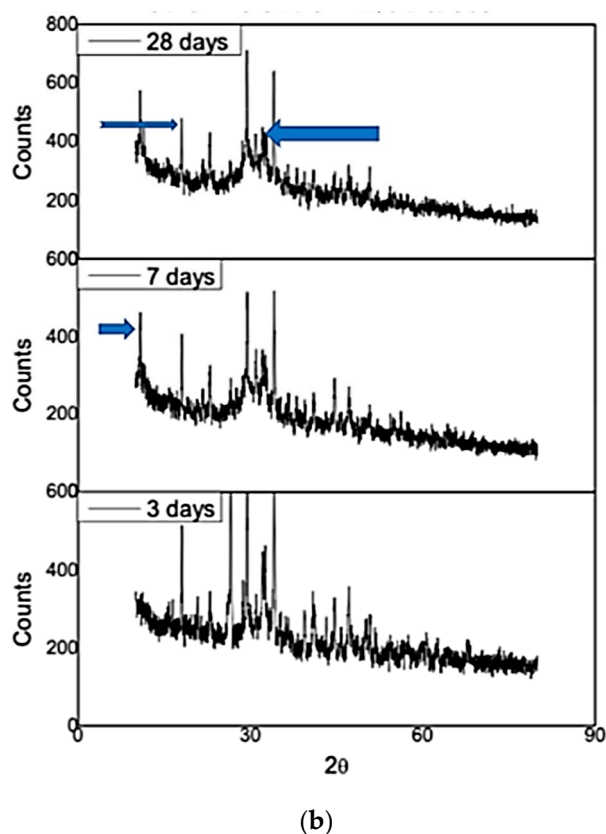


Figure 9. Cont.



**Figure 9.** X-ray diffraction patterns of the specimen (a) OPC+GGBS Mix Series specimen (OPGG CON-1), (b) OPC+GGBS Mix Series specimen with 2% innovative additive (OPGGNA-4).

Figure 10 presents the Scanning Electron Microscopy (SEM) images of the microstructure for two specimens of OPC+GGBS Mix Series concrete, showing notable differences in microstructural features based on the presence of the innovative additive.

In Figure 10a, the SEM image of the reference specimen (OPGG CON-1) without the innovative additive reveals a relatively loose and porous microstructure. There are noticeable large holes and microcracks, which point to inadequate packing density and inadequate hydration. These voids may indicate a weaker matrix overall and a greater chance of water penetration, which could result in decreased mechanical strength and durability. The microstructure appears fragmented, with poorly bonded hydration products, consistent with a typical OPC+GGBS mix at an early hydration stage, where unreacted materials remain.

In contrast, Figure 10b, which shows the SEM image of the specimen containing 2% innovative additive (OPGGNA-4), displays a more compact and well-developed microstructure. The image shows a denser, more continuous matrix structure with fewer voids and cracks. This suggests that the novel addition has improved particle bonding and the cohesive production of calcium silicate hydrate (C-S-H) gels by positively impacting the hydration process. The improved microstructure points to enhanced mechanical performance, as the denser packing reduces porosity and increases the strength and durability of the concrete. These findings align with the XRD results, which suggested a higher degree of pozzolanic activity and a more complete consumption of calcium hydroxide (CH) in the presence of the innovative additive.

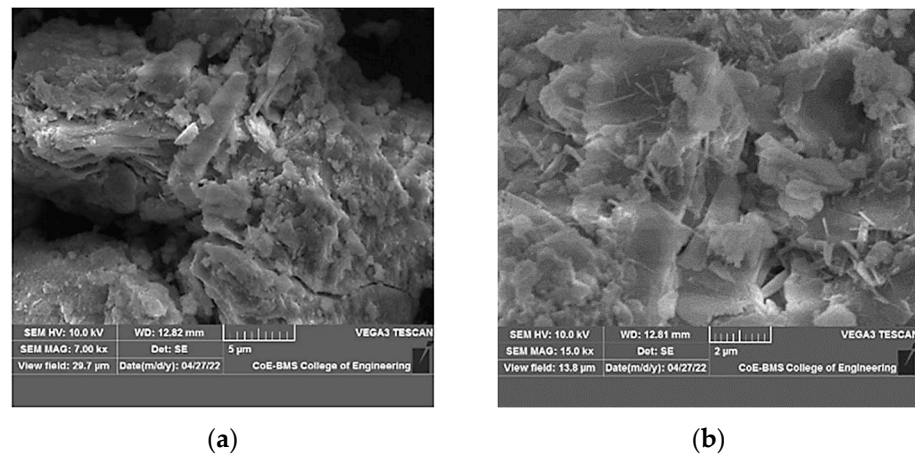


**Figure 10.** SEM of the specimen (a) OPC+GGBS Mix Series specimen (OPGG CON-1), (b) OPC+GGBS Mix Series specimen with 2% innovative additive (OPGGNA-4).

### 3.4. Corrosion Behavior of Embedded Steel Reinforcement

#### 3.4.1. Impact of Chemical Admixtures on Corrosion of Embedded Steel Reinforcement in Concrete Using Macrocell Corrosion Testing

Table 6 presents the corrosion potential values for two concrete specimens—one with the ICRETE mineral additive and one without it. Measurements were taken at intervals of 0, 7, and 14 days to monitor the corrosion progression over time. According to ASTM C876, potential values less negative than  $-125$  mV indicate a low probability of corrosion, whereas values between  $-125$  mV and  $-275$  mV suggest an uncertain corrosion condition. On day 14, the specimen without ICRETE had a potential of  $-128$  mV, indicating a passive or uncertain state, while the specimen with ICRETE showed a potential of  $-109$  mV, suggesting enhanced corrosion resistance compared to the specimen without the additive. These data highlight the potential benefits of the ICRETE additive in reducing the risk of corrosion in reinforced concrete.

**Table 6.** Potential value for concrete specimens with and without ICRETE mineral additive.

Specimen ID/No. of Days	Potential (mV) vs. SCE		
	0 Days	7 Days	14 Days
Without ICRETE (OP CON-1)	$-116$	$-154$	$-128$
With ICRETE (OPNA-2)	$-76$	$-148$	$-109$

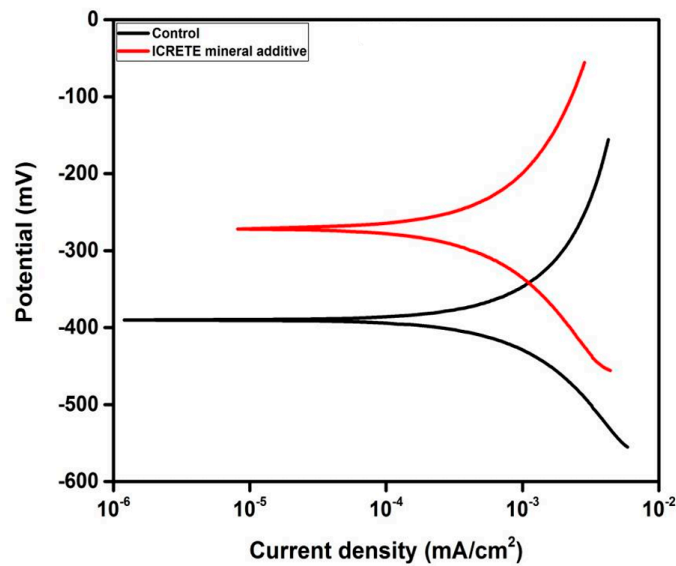
#### 3.4.2. Corrosion Behavior by Electrochemical Studies

Table 7 provides the corrosion kinetic parameters for concrete specimens with and without the ICRETE mineral additive. The specimen with ICRETE shows a lower corrosion current density ( $I_{corr}$ ) and corrosion rate than the specimen without ICRETE, indicating improved corrosion resistance.

**Table 7.** Corrosion kinetic parameters for rebar embedded in concretes with and without ICRETE mineral additive.

System	OCP (mV vs. SCE)	E <sub>corr</sub> (mV vs. SCE)	I <sub>corr</sub> (mA/cm <sup>2</sup> )	Corrosion Rate (mm/year)
Without ICRETE	$-328$	$-389$	0.0009	0.0100
With ICRETE	$-267$	$-270$	0.0007	0.0081

As illustrated in Figure 11, the polarization curve highlights the reduction in corrosion activity using the ICRETE additive, supporting its effectiveness in enhancing concrete durability. Figure 11 shows two branches for each curve: an upward branch representing anodic polarization (where the steel rebar undergoes oxidation, contributing to corrosion) and a downward branch representing cathodic polarization (indicating reduction reactions, such as oxygen reduction). The shift in the red curve, corresponding to concrete with ICRETE, demonstrates a lower corrosion current density and more positive potential compared to the control (black curve). This indicates that the ICRETE additive effectively suppresses both anodic and cathodic reactions, reducing the overall corrosion rate and enhancing the long-term durability of steel-reinforced concrete.



**Figure 11.** Potentiodynamic polarization curve for steel rebar embedded in concrete with and without (control) ICRETE mineral additive.

✿ **Linear polarization resistance**

Table 8 presents the polarization resistance ( $R_p$ ) values for concrete specimens with and without the ICRETE mineral additive.

**Table 8.** Polarization resistance ( $R_p$ ) values.

System	$R_p$ (Ohm·cm <sup>2</sup> )
Without ICRETE	33,053
With ICRETE	43,204

As shown in Figure 12, the Linear Polarization Resistance (LPR) plots illustrate that the specimen with ICRETE has a higher  $R_p$  value than the control (without ICRETE). The  $R_p$  value increased from 33,053 ohm·cm<sup>2</sup> in the control specimen to 43,204 ohm·cm<sup>2</sup> with the ICRETE additive, indicating enhanced corrosion resistance. This significant increase in  $R_p$  suggests that the ICRETE mineral additive improves the durability of the steel reinforcement in concrete, further supporting its effectiveness in mitigating corrosion.

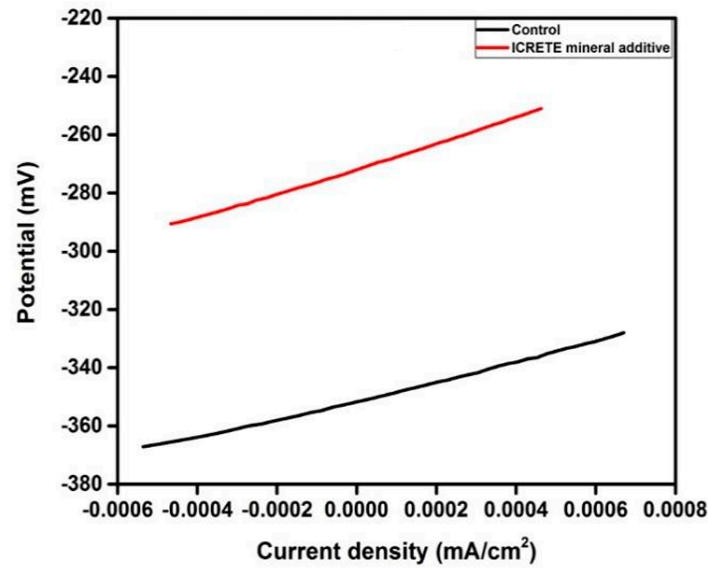


Figure 12. LPR plots for steel rebar embedded in concrete with and without (control) ICRETE mineral additive.

✿ Electrochemical impedance spectroscopy

Figure 13 shows the impedance of Bode’s plot for steel rebar embedded in concrete with and without the ICRETE mineral additive. At a frequency of 0.1 Hz, the impedance for the specimen with ICRETE is 41,056 ohm·cm<sup>2</sup>, compared to 34,571 ohm·cm<sup>2</sup> for the specimen without ICRETE. This increase in impedance with the ICRETE additive indicates enhanced corrosion resistance, as higher impedance values generally correlate with a reduced corrosion rate.

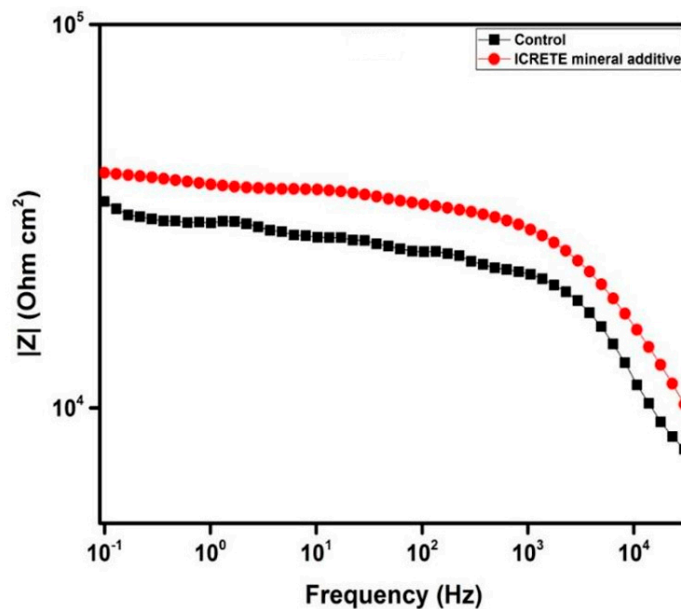


Figure 13. Bode’s plots for steel rebar embedded in concrete with and without (control) ICRETE mineral additive.

4. Environmental Impact, Cost Analysis, and Durability Assessment of Concrete Mixes Using the Innovative Additive

The environmental impact of the innovative additive used in various concrete mix series was assessed by calculating CO<sub>2</sub> emissions reductions resulting from decreased cement

content. This research utilized a detailed and accurate method provided by the Circular Ecology Concrete Embodied Carbon Footprint Calculator, available on this website [29].

This tool allows for selecting specific cement types, including Cement CEM I—Portland cement, Cement CEM II/B-S—28% GGBS, Portland slag cement, and others. The calculator provides a tailored calculation of the embodied carbon footprint by entering the exact quantities of cement, GGBS, fly ash, and other supplementary cementitious materials (SCMs). Additionally, the tool considers the water-to-cement ratio, which is a crucial factor in determining the environmental impact of the concrete mix.

In the process, the following steps were performed:

✿ **Selection of Cement Type:**

The calculator allows for selecting specific cement types relevant to each mix design. For instance, “Cement CEM I—Portland cement” was chosen for mixes primarily using Portland cement, while other options such as “Cement CEM II/B-S—28% GGBS, Portland-slag cement” were used where applicable.

✿ **Entry of Cementitious Materials:**

The calculator entered each mix’s precise PFA, GGBS, and cement (OPC) amounts. This ensures that the actual mix composition, rather than a generic factor, is used to calculate the embodied carbon footprint. Supplemental cementitious materials (SCMs) like GGBS and PFA can significantly reduce the carbon footprint due to their reduced related emissions compared to traditional OPC.

✿ **Water-to-Cement Ratio:**

The calculator was also used to enter the water-to-cement (w/c) ratio, a crucial element for assessing the mix’s environmental impact. This ratio affects the concrete’s overall carbon footprint, strength, and durability because water processing uses energy and impacts the concrete’s hydration process.

✿ **Total Admixtures and Aggregates:**

The calculator also includes fields for entering the total amount of admixtures and aggregates used in the concrete mix. This is important as the production and transportation of these materials contribute to the overall embodied carbon footprint. The exact quantities of coarse and fine aggregates were entered to ensure an accurate calculation of the total material footprint.

✿ **In situ or Precast Selection:**

The environmental impact differs based on whether the concrete is used in situ (cast in place) or precast applications. The calculator allows for selecting these options, which was used to adjust the calculation accordingly. In this study, the type of concrete (in situ or precast) was selected based on the intended application of each mix, further refining the environmental impact assessment.

✿ **Calculation of Embodied Carbon:**

After entering all the necessary inputs, the calculator provided a detailed calculation of each concrete mix’s embodied carbon footprint. This included the emissions associated with cement production, the contributions from SCMs, water, admixtures, and aggregates, and the energy required for in situ or precast construction processes.

The results presented in Table 9 demonstrate significant reductions in CO<sub>2</sub> emissions achieved using the innovative additive across all concrete mix series. In the OPC Mix Series, the addition of the innovative additive led to a maximum CO<sub>2</sub> emissions reduction of 46.50 kg CO<sub>2</sub>/m<sup>3</sup> for the mix with 1.2% additive dosage (OPNA-2), directly correlated with the decreased cement content, allowing for the production of concrete with lower cement content without compromising strength. The OPC+GGBS Mix Series showed a maximum reduction of 25.50 kg CO<sub>2</sub>/m<sup>3</sup> for the mix with 1.2% additive dosage (OPGGNA-2), with the use of GGBS as a partial replacement for OPC further contributing to the lower carbon footprint. Similarly, the OPC+PFA Mix Series 1 achieved a maximum reduction of 38.10 kg

CO<sub>2</sub>/m<sup>3</sup> with the 1.2% additive dosage (OPCFLYNA-2), highlighting the environmental benefits of incorporating PFA to lower cement content and emissions. In the OPC+PFA Mix Series 2, the mix with 1.2% additive dosage (OPCFLYNA-7) achieved a reduction of 32.22 kg CO<sub>2</sub>/m<sup>3</sup>, with the higher PFA content further reducing the reliance on OPC, leading to significant environmental savings. Overall, the use of the innovative additive in combination with SCMs like GGBS and PFA results in considerable reductions in CO<sub>2</sub> emissions across various concrete mix designs, confirming the additive’s effectiveness in producing more sustainable concrete and promoting greener construction practices.

**Table 9.** CO<sub>2</sub> Emissions and Cost Reductions Achieved with the Innovative Additive Across Various Concrete Mix Series.

Mix Series	Mix Description	Cement Content (kg/m <sup>3</sup> )	CO <sub>2</sub> Emissions (kg CO <sub>2</sub> /m <sup>3</sup> )	Reduction (kg CO <sub>2</sub> /m <sup>3</sup> )	Total Cost (USD/m <sup>3</sup> )	Cost Reduction (USD/m <sup>3</sup> )
OPC Mix Series	OP CON-1 (Control)	450	418.50	-	37.75	0.00
	OPNA-1 (0.8%)	425	395.25	23.25	38.68	-0.93
	OPNA-2 (1.2%)	400	372.00	46.50	38.89	-1.14
OPC+GGBS Mix Series	OPGG CON-1 (Control)	225 OPC + 225 GGBS	229.50	-	33.44	4.31
	OPGGNA-1 (0.8%)	212.5 OPC + 212.5 GGBS	216.75	12.75	34.47	3.28
	OPGGNA-2 (1.2%)	200 OPC + 200 GGBS	204.00	25.50	34.96	2.79
OPC+PFA Mix Series 1	OPFLY CON-1 (Control)	360 OPC + 90 PFA	342.90	-	36.24	1.51
	OPCFLYNA-1 (0.8%)	340 OPC + 85 PFA	323.85	19.05	37.23	0.52
	OPCFLYNA-2 (1.2%)	320 OPC + 80 PFA	304.80	38.10	36.93	0.82
OPC+PFA Mix Series 2	OPCFLYNA-2 (Control)	293 OPC + 157 PFA	286.62	-	34.91	2.84
	OPCFLYNA-6 (0.8%)	276 OPC + 149 PFA	270.09	16.53	35.67	2.08
	OPCFLYNA-7 (1.2%)	260 OPC + 140 PFA	254.40	32.22	35.89	1.86

The cost analysis has also been carried out to evaluate the economic implications of different concrete mixes, with the results presented in the Total Cost (USD/m<sup>3</sup>) and Cost Reduction (USD/m<sup>3</sup>) columns. These values were calculated based on the material prices provided: cement (USD 55/ton), fly ash (USD 20/ton), GGBS (USD 40–45/ton), Icrete (USD 400/ton), and aggregates (USD 8–9/ton). The Total Cost (USD/m<sup>3</sup>) reflects the material cost for each mix, while the Cost Reduction (USD/m<sup>3</sup>) highlights the savings achieved compared to the control mix (OP CON-1). The analysis demonstrates that incorporating supplementary cementitious materials, such as GGBS and fly ash, alongside the innovative additive Icrete, can lead to significant cost reductions. For instance, OPGG CON-1, which replaces 50% of cement with GGBS, reduced the cost by USD 4.31/m<sup>3</sup>, while OPCFLYNA-2, containing 20% fly ash and 1.2% Icrete, achieved a reduction in USD 0.82/m<sup>3</sup>.

Concrete structures are often subjected to aggressive environmental conditions that significantly impact their durability and longevity. One of the critical factors affecting the durability of concrete is its resistance to expansion and cracking when exposed to harsh environments such as sulfate-rich soils and seawater. Expanding concrete due to sulfate attack and other environmental factors can lead to structural deterioration and a reduction in service life. In this study, the effectiveness of an innovative additive in enhancing the resistance of concrete to such environmental stressors was evaluated. Various

concrete mixes' performance was assessed over a prolonged period of 378 days. The expansion behavior of the concrete mixes was monitored to determine the additive's impact on mitigating the harmful effects of environmental exposure. Figures 14 and 15 present the results of this investigation, highlighting the varying degrees of expansion among the different mix series and demonstrating the additive's potential to produce more durable concrete.

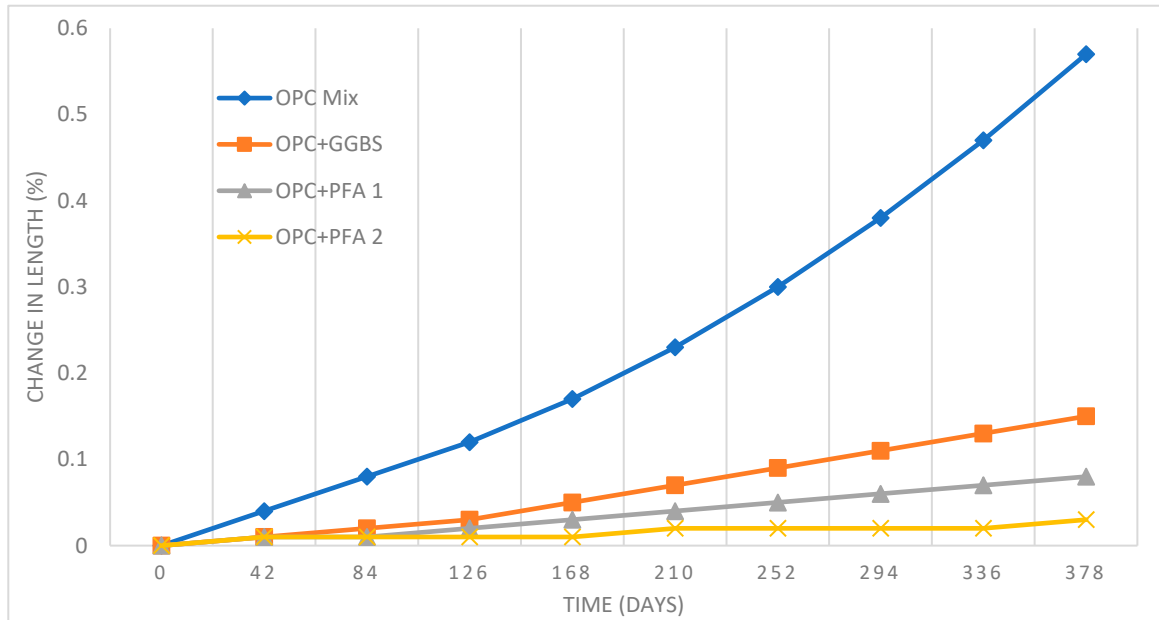


**Figure 14.** Expansion behavior of various concrete mixes immersed in a 5% Na<sub>2</sub>SO<sub>4</sub> solution over 378 days.

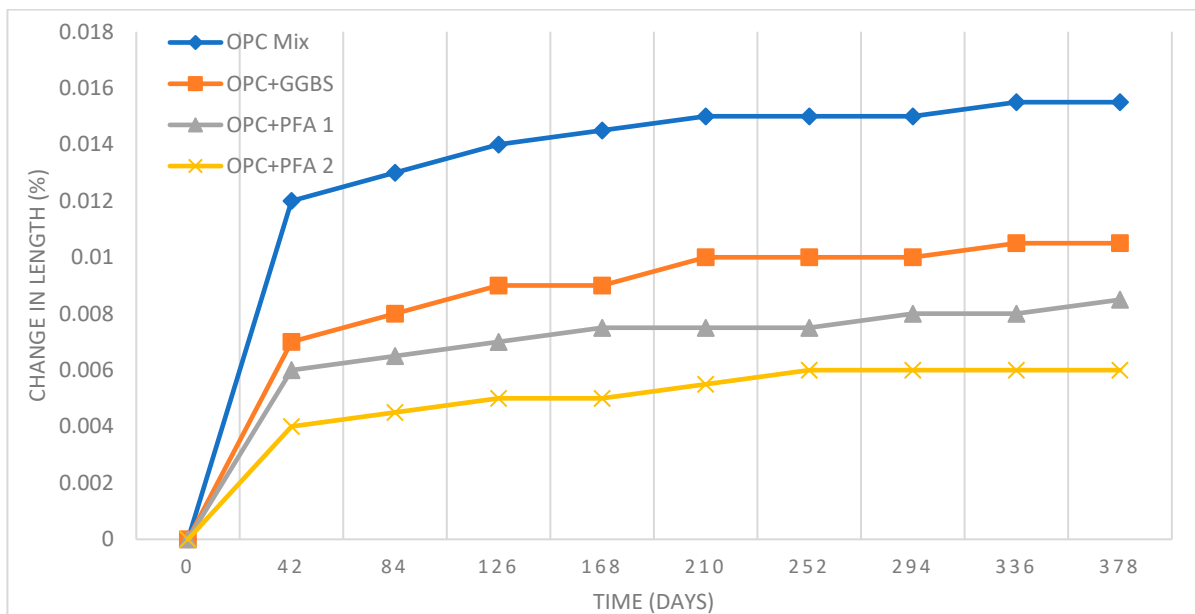


**Figure 15.** Expansion behavior of various concrete mixes exposed to seawater over 378 days.

Figure 14 presents the expansion behavior of concrete samples immersed in a 5% Na<sub>2</sub>SO<sub>4</sub> solution over 378 days. The OPC Mix Series, serving as the control, exhibits the most significant expansion, reaching approximately 0.57% after 12 months, indicating significant vulnerability to sulfate attacks. In contrast, the OPC+GGBS Mix Series shows

a substantial reduction in expansion, with a maximum expansion of around 0.31%. The OPC+PFA Mix Series 1 and OPC+PFA Mix Series 2 demonstrate further improvements in sulfate resistance, with expansions of 0.14% and 0.08%, respectively. These lower expansion values suggest that using PFA, especially in higher dosages, considerably enhances the sulfate resistance of concrete, outperforming the control mix significantly.

Figure 15 illustrates the expansion of concrete samples exposed to seawater over 378 days. The control mix (OPC Mix Series) shows the highest expansion, peaking at about 0.0155%, reflecting poor resistance to the harsh seawater environment. Including GGBS in the OPC+GGBS Mix Series reduces the expansion to approximately 0.0105%. The OPC+PFA Mix Series 1 and OPC+PFA Mix Series 2 display even lower expansions, with maximum values of 0.0085% and 0.006%, respectively. These results confirm the efficacy of the innovative additive in enhancing the sulfate resistance of concrete, particularly when PFA is used, significantly reducing the expansion compared to the control mix.

## 5. Concluding Remarks

In this section, the study's key findings and implications are summarized. The results demonstrate the effectiveness of the innovative additive in enhancing the performance and sustainability of concrete mixes. Below are the main conclusions drawn from the research:

- i. **Enhanced Compressive Strength:** The inclusion of the innovative additive in concrete mixes significantly improved compressive strength. For instance, the OPC Mix Series with 0.8% additive dosage (OPNA-1) achieved a compressive strength of 56.93 MPa, surpassing the control mix's strength of 50.9 MPa. This demonstrates the additive's ability to maintain or even enhance strength levels at reduced cement contents.
- ii. **Environmental Impact:** The study highlights the innovative additive's environmental benefits. In the OPC Mix Series, a maximum reduction of 46.50 kg CO<sub>2</sub>/m<sup>3</sup> was observed with a 1.2% additive dosage (OPNA-2). Similarly, the OPC+GGBS and OPC+PFA Mix Series showed reductions of 25.50 kg CO<sub>2</sub>/m<sup>3</sup> and 38.10 kg CO<sub>2</sub>/m<sup>3</sup>, respectively. These findings indicate that the additive significantly contributes to reducing the carbon footprint of concrete production.
- iii. **Durability and Sulfate Resistance:** The additive demonstrated its efficacy in enhancing the durability of concrete, particularly in terms of sulfate resistance. The OPC Mix Series exhibited the highest expansion in sulfate environments, whereas the inclusion of GGBS and PFA in the OPC+GGBS and OPC+PFA Mix Series significantly reduced expansion, enhancing the concrete's sulfate resistance.
- iv. **Corrosion mitigation:** The specimen with ICRETE demonstrated a significantly lower corrosion current density (*I*<sub>corr</sub>) and corrosion rate compared to the specimen without ICRETE, with reductions from 0.0009 mA/cm<sup>2</sup> to 0.0007 mA/cm<sup>2</sup> and from 0.0100 mm/year to 0.0081 mm/year, respectively. This indicates that the ICRETE mineral additive effectively mitigates corrosion in concrete.
- v. **Enhanced durability:** Impedance measurements at 0.1 Hz revealed that the specimen with ICRETE achieved a higher impedance value of 41,056 ohm·cm<sup>2</sup>, compared to 34,571 ohm·cm<sup>2</sup> for the specimen without ICRETE, suggesting enhanced durability and resistance to corrosion in the ICRETE-modified concrete.
- vi. **Microstructural Improvements:** Microstructural analysis through SEM and XRD confirmed that the innovative additive promotes the formation of denser and more homogeneous hydration products. This leads to reduced porosity and improved durability, which are critical for the long-term performance of concrete in various environmental conditions.

Future studies should focus on optimizing the dosage of the innovative additive across a broader range of cementitious materials and environmental conditions. This could include exploring the additive's performance in extreme climates, varying exposure conditions, and with different types of supplementary cementitious materials (SCMs).

**Author Contributions:** Conceptualization, K.V., V.B. and R.N.; methodology, K.V. and R.N.; validation, K.V., V.B. and I.F.; writing—original draft, K.V.; writing—review and editing, I.F.; supervision, I.F. All authors have read and agreed to the published version of the manuscript.

**Funding:** This research received no external funding.

**Data Availability Statement:** Data are contained within the article.

**Acknowledgments:** We Thank the International School of Management Excellence, Research Centre affiliated to the University of Mysore, for their administrative support. This research project is self-funded; no organization has funded it.

**Conflicts of Interest:** Author Ramkumar Natarajan was employed by the company Navoday Sciences Private Limited. The remaining authors declare that the research was conducted in the absence of any commercial or financial relationships that could be construed as a potential conflict of interest.

## References

1. Plank, J.; Ilg, M. The role of chemical admixtures in the formulation of modern advanced concrete. In *3rd International Conference on the Application of Superabsorbent Polymers (SAP) and Other New Admixtures Towards Smart Concrete 3*; Springer: New York, NY, USA, 2020.
2. Kondraivendhan, B.; Bhattacharjee, B. Strength and w/c ratio relationship of cement based materials through pore features. *Mater. Charact.* **2016**, *122*, 124–129. [[CrossRef](#)]
3. Nikbin, I.; Beygi, M.; Kazemi, M.; Amiri, J.V.; Rabbanifar, S.; Rahmani, E.; Rahimi, S. A comprehensive investigation into the effect of water to cement ratio and powder content on mechanical properties of self-compacting concrete. *Constr. Build. Mater.* **2014**, *57*, 69–80. [[CrossRef](#)]
4. Łagosz, A.; Olszowski, D.; Pichór, W.; Kotwica, Ł. Quantitative determination of processed waste expanded perlite performance as a supplementary cementitious material in low emission blended cement composites. *J. Build. Eng.* **2021**, *40*, 102335. [[CrossRef](#)]
5. Capacchione, C.; Partschefeld, S.; Osburg, A.; Gliubizzi, R.; Gaeta, C. Modified carboxymethylcellulose-based scaffolds as new potential ecofriendly superplasticizers with a retardant effect for mortar: From the synthesis to the application. *Materials* **2021**, *14*, 3569. [[CrossRef](#)] [[PubMed](#)]
6. Hedegaard, S.E.; Hansen, T.C. Water permeability of fly ash concretes. *Mater. Struct.* **1992**, *25*, 381–387. [[CrossRef](#)]
7. Hosseinzadehfard, E.; Mobaraki, B. Investigating concrete durability: The impact of natural pozzolan as a partial substitute for microsilica in concrete mixtures. *Constr. Build. Mater.* **2024**, *419*, 135491. [[CrossRef](#)]
8. Khan, K.; Ullah, M.F.; Shahzada, K.; Amin, M.N.; Bibi, T.; Wahab, N.; Aljaafari, A. Effective use of micro-silica extracted from rice husk ash for the production of high-performance and sustainable cement mortar. *Constr. Build. Mater.* **2020**, *258*, 119589. [[CrossRef](#)]
9. Tabish, M.; Zaheer, M.M.; Baqi, A. Effect of nano-silica on mechanical, microstructural and durability properties of cement-based materials: A review. *J. Build. Eng.* **2023**, *65*, 105676. [[CrossRef](#)]
10. Mehta, P.K.; Monteiro, P. *Concrete: Microstructure, Properties, and Materials*, 3rd ed.; McGraw-Hill Education: New York, NY, USA, 2006.
11. Najjar, M.F.; Soliman, A.M.; Nehdi, M.L. Critical overview of two-stage concrete: Properties and applications. *Constr. Build. Mater.* **2014**, *62*, 47–58. [[CrossRef](#)]
12. Fu, Q.; Zhao, X.; Zhang, Z.; Xu, W.; Niu, D. Effects of nanosilica on microstructure and durability of cement-based materials. *Powder Technol.* **2022**, *404*, 117447. [[CrossRef](#)]
13. Gill, A.S.; Siddique, R. Strength and micro-structural properties of self-compacting concrete containing metakaolin and rice husk ash. *Constr. Build. Mater.* **2017**, *157*, 51–64. [[CrossRef](#)]
14. Hardened Concrete—Methods of Test, Part 2: Properties of Hardened Concrete Other than Strength, Section 1: Density of Hardened Concrete and Depth of Water Penetration Under Pressure. Available online: <https://www.scribd.com/document/476387798/IS-516-Part-2-Sec-1-2018> (accessed on 6 December 2024).
15. Concrete Mix Proportioning—Guidelines (Second Revision). Available online: <https://archive.org/details/gov.in.is.10262.2019/mode/2up> (accessed on 6 December 2024).
16. Indian Standard, Plain and Reinforced Concrete—Code of Practice (Fourth Revision). Available online: <https://law.resource.org/pub/in/bis/S03/is.456.2000.pdf> (accessed on 6 December 2024).
17. Varghese, P. *Limit State Design of Reinforced Concrete*; PHI Learning Pvt. Ltd.: Delhi, India, 2008.
18. Bureauofindianstandar, D. *Coarse and Fine Aggregate for Concrete Specification*; BIS: Delhi, India, 2016.
19. Ordinary Portland Cement—Specification (Sixth Revision). Available online: <https://www.scribd.com/document/690243322/IS-269-2015-Reaffirmed-2020> (accessed on 6 December 2024).
20. Harish, B.; Dakshinamurthy, N.; Sridhar, M.; Rao, K.J. A study on mechanical properties of high strength concrete with alccofine as partial replacement of cement. *Mater. Today Proc.* **2022**, *52*, 1201–1210. [[CrossRef](#)]

21. Kamplimath, H.; Dave, U.V.; Kothari, V. Evaluation of Mechanical Properties of Sustainable Concrete Pavement Utilizing Medium-to High-Volume Ground-Granulated Blast Furnace Slag. In *Advances in Sustainable Construction Materials: Select Proceedings of ASCM 2020*; Springer: New York, NY, USA, 2021; pp. 37–46.
22. Abualrous, Y. *Characterization of Indian and Canadian Fly Ash for Use in Concrete*; University of Toronto: Toronto, ON, Canada, 2017.
23. Standard Test Methods for Determining Effects of Chemical Admixtures on Corrosion of Embedded Steel Reinforcement in Concrete Exposed to Chloride Environments. Available online: <https://www.astm.org/g0109-21.html> (accessed on 6 December 2024).
24. Wang, J.; Wang, Q.; Zhao, Y.; Li, P.; Ji, T.; Zou, G.; Qiao, Y.; Zhou, Z.; Wang, G.; Song, D. Research Progress of Macrocell Corrosion of Steel Rebar in Concrete. *Coatings* **2023**, *13*, 853. [[CrossRef](#)]
25. Ramírez, G.P.M.; Baltazar-Zamora, M.A.; Ramírez, C.T.M.; Niedostatkiewicz, M.; Byliński, H. Corrosion of AISI1018 and AISI304 steel exposed to sulfates. *Inżynieria Bezpieczeństwa Obiektów Antropog.* **2024**, *3*, 58–70. [[CrossRef](#)]
26. Xia, D.-H.; Deng, C.-M.; Macdonald, D.; Jamali, S.; Mills, D.; Luo, J.-L.; Strebl, M.G.; Amiri, M.; Jin, W.; Song, S.; et al. Electrochemical measurements used for assessment of corrosion and protection of metallic materials in the field: A critical review. *J. Mater. Sci. Technol.* **2022**, *112*, 151–183. [[CrossRef](#)]
27. Anita, N.; Joany, R.M.; Dorothy, R.; Aslam, J.; Rajendran, S.; Subramania, A.; Singh, G.; Verma, C. Linear polarization resistance (LPR) technique for corrosion measurements. In *Electrochemical and Analytical Techniques for Sustainable Corrosion Monitoring*; Elsevier: Amsterdam, The Netherlands, 2023; pp. 59–80.
28. Magar, H.S.; Hassan, R.Y.A.; Mulchandani, A. Electrochemical Impedance Spectroscopy (EIS): Principles, Construction, and Biosensing Applications. *Sensors* **2021**, *21*, 6578. [[CrossRef](#)] [[PubMed](#)]
29. Joensuu, T.; Leino, R.; Heinonen, J.; Saari, A. Developing Buildings' Life Cycle Assessment in Circular Economy-Comparing methods for assessing carbon footprint of reusable components. *Sustain. Cities Soc.* **2022**, *77*, 103499. [[CrossRef](#)]

**Disclaimer/Publisher's Note:** The statements, opinions and data contained in all publications are solely those of the individual author(s) and contributor(s) and not of MDPI and/or the editor(s). MDPI and/or the editor(s) disclaim responsibility for any injury to people or property resulting from any ideas, methods, instructions or products referred to in the content.